

# Response Function of an Irregular Oscillator

Hirokazu Aiba<sup>1</sup>, and Toru Suzuki<sup>2</sup>

<sup>1</sup>*Koka Women's College, 38 Kadono-cho Nishikyogoku, Ukyo-ku, 615-0882 Kyoto, Japan*

<sup>2</sup>*Department of Physics, Tokyo Metropolitan University, 192-0397 Hachioji, Japan*

(March 21, 2022)

Properties of the response functions for a two-dimensional quartic oscillator are studied based on the diagonalization of the Hamiltonian in a large model space. In particular, response functions corresponding to a given momentum transfer are studied for different values of the coupling parameter in the Hamiltonian. The latter controls regular or chaotic nature of the spectra and eigenstates of the system. Fluctuation properties of the energy-strength correlation of the response are investigated. Even when the statistical properties of the system indicate an almost completely chaotic character, there remains a typical structure in the response function similar to that in the regular system. The nature of this structure is studied in some detail.

PACS number: 05.45.Mt, 05.40.-a, 05.45.-a

## I. INTRODUCTION

Quantum mechanical manifestations of dynamical properties of a system which classically possesses a chaotic character have been intensively studied [1,2]. Level statistics which has a long history in nuclear physics as described by the random-matrix theory [3,4] is now a favorable playground in the discussion of a transition from a regular (integrable) to a chaotic character of a quantum system. Together with numerical studies on model systems, analytic investigation has been made based on semiclassical trace formula [5]. Wave functions of a system which is classically chaotic have also been investigated: Statistical theory predicts that the amplitude distributions show the Porter-Thomas distribution [6], which was then numerically demonstrated to hold for model chaotic systems. Contrary to the naive expectation, however, the profile of the wave function for a chaotic system is not entirely structureless: For instance, the Husimi representation of a wave function in the chaotic regime frequently suffers from a *scar* of classical periodic orbits [7]. Although a considerable progress has since been made, it is still an important issue to clarify the characteristic of eigenstates and its matrix elements for systems which are classically irregular or chaotic.

It is the purpose of the present paper to study another aspect of the wave functions for a system which shows a transition from an integrable to a chaotic character: We study response functions of the system, i.e. transition matrix elements as a function of energy. Statistical properties of the distribution of transition matrix elements have been studied [8–10], and it was shown, in particular, that the distribution becomes a Porter-Thomas type for chaotic systems. The approach proposed in Ref. [10] has since been developed to elucidate the role of periodic orbits and was extended to various systems including the response of mesoscopic systems to realistic probes [11–14]. These studies are based on the semiclassical framework, and focus mainly on the responses to long-wavelength probes. Semiclassical studies of response functions have also been done in a different framework [15], which concentrate on their smooth behavior but not much on fluctuations.

In this paper, we study a model system using a large space diagonalization and calculating response functions for the operators which probe the system with a variable wavelength, or momentum transfer. In particular, we put an emphasis on which aspect of the response function reflects the regular or the chaotic character of the system. We also would like to study a structure in the response function for a system in a chaotic regime which however is not expected to occur in the statistical random-matrix theory. Although we are here concerned with the properties of response functions which show up in a model system, they will also be interesting in realistic applications, as this response is similar to the excitation cross section for, e.g., electron scattering in the plane-wave Born approximation. Thus it is hoped that the present study may provide insight into the understanding of collective states such as nuclear giant resonances embedded in complicated many-particle many-hole states as studied in nuclear reactions.

The main content of the paper is as follows: In the next section we summarize classical and quantum mechanical properties of the model Hamiltonian and fix values of the relevant parameters. In Sec. III we study response functions first for a long wavelength probe, and then for the probe characterized by a given momentum transfer. We study the fluctuation properties of the response functions, concentrating especially on the similarity or the difference for the regular and the chaotic systems. The accuracy of the calculation has been checked against sum rules. Final section is devoted to a summary.

## II. BASIC INGREDIENTS OF THE MODEL

In order to study the response functions for a system which is capable of showing regular as well as chaotic properties, we adopt the following Hamiltonian as a model,

$$H = \frac{1}{2}(p_x^2 + p_y^2) + \frac{1}{2}(x^4 + y^4) - kx^2y^2. \quad (1)$$

This model Hamiltonian has been adopted by a number of authors for the studies of level statistics or wave functions [17–21]. It was also employed as a model for a background system in the studies of the fluctuation properties of strength functions. [22] Let us first briefly summarize classical properties of the model, which have been studied in detail by Meyer [18]. The Hamiltonian (1) possesses a dynamical scaling property in the sense that the classical phase space structure at one energy is mapped into another by a simple scaling of the coordinates and momenta. It has a high symmetry called  $C_{4v}$ : The Hamiltonian is invariant with respect to a reflection about  $x$ -axis,  $y$ -axis, and also about the line  $x = y$ . Furthermore, by rotating  $45^\circ$  in the  $x - y$  plane, the Hamiltonian is mapped into the one with a coupling constant  $k' = -(3 + k)/(1 - k)$ . As the system becomes unbounded from below for  $k > 1$ , we have only to consider the range  $[-1, 1]$  for the coupling constant  $k$ . Meyer [18] showed that for large  $k$  values ( $\geq 0.4$ ) the classical phase space structure is almost completely chaotic, while for small  $k$  the system becomes regular. In the following calculations we adopt two typical values of the parameter:  $k = 0.2$  and  $0.6$ . They correspond to quasiintegrable and fully chaotic systems, respectively. For instance, for  $k = 0.6$  a single trajectory fills up almost 90% of the available phase space, while for  $k = 0.2$  the fraction of the phase space covered by irregular orbits is only 25% in typical cases [18].

To study quantum mechanical properties of the eigenstates of the Hamiltonian (1), we follow the procedure essentially of Zimmerman et al. [19]: The Hamiltonian is diagonalized within a truncated model space spanned by a set of suitable harmonic oscillator bases  $|n_x, n_y\rangle$ , where  $n_x, n_y$  denote the numbers of oscillator quanta in the  $x$ - and  $y$ -directions. In the following we take the unit  $\hbar = 1$ . The frequency  $\omega_0$  of the harmonic oscillator basis is determined so as to minimize  $\text{tr}H$  in the adopted model space. The obtained values of  $\omega_0$  are  $7.51(k = 0.2)$  and  $7.13(k = 0.6)$ . The Hamiltonian matrix can be decomposed into submatrices due to the  $C_{4v}$  symmetry. As in Ref. [20] we take up four classes of the one-dimensional representation which are labeled as  $A_1, A_2, B_1, B_2$  according to their symmetry properties under reflection on the axes and diagonals in the  $x - y$  plane [18]. (For instance,  $A_1$  is symmetric under both reflections.) The model space is spanned by the bases with  $0 \leq n_x + n_y \leq 300$ , which gives the dimension of each submatrices as 5776, 5625, 5700, 5700. The diagonalization has been performed for each submatrices. Study of the nearest-neighbor spacing distribution confirms the character of the system suggested by the classical phase space structures, i.e., the Poisson like distribution for  $k = 0.2$  and the Wigner distribution for  $k = 0.6$  within each symmetry class. We also confirmed that the amplitude distribution of the wave functions for  $k=0.6$  show the Porter-Thomas distribution except for a singular peak at zero.

In the following the results of the calculation will be shown for the states which belong to the symmetry class  $A_1$ . The results are similar for other symmetry classes.

The basis state  $|n_1, n_2\rangle_{\text{ES}}$  belonging to the class  $A_1$  is written as

$$|n_1, n_2\rangle_{\text{ES}} = \sqrt{\frac{1 + \delta_{n_1 n_2}}{2}}(|n_1, n_2\rangle + |n_2, n_1\rangle), \quad (2)$$

where  $n_1$  and  $n_2$  are even integers and  $n_1 \leq n_2$ . Because of the selection rule, the relevant part of the operator which contributes to the matrix element of the response should have the definite symmetry property. It should be noted that among the 5776 wave functions of the class  $A_1$ , those having very large energies are not quite reliable because of the limitation in the basis states. This is especially so when the response functions with large momentum transfer  $q$  are concerned. We may make an estimate for the range of validity by comparing the obtained level density with the semiclassical one. The comparison suggests that the maximum reliable energy to be  $E = 1000 \sim 1500$  depending on the values of the parameter  $k$  in Eq. (1). This maximum energy is contrasted with the largest energy eigenvalue  $E \simeq 3000$  obtained by the diagonalization. This limits the maximum value of the momentum transfer of the probe adopted below to be around  $q \simeq 50$ , where the corresponding ‘quasielastic peak’ lies around  $E_{\text{peak}} = q^2/2 \simeq 1250$ . This is confirmed by the calculation as shown later.

## III. RESPONSE FUNCTIONS

We consider the response functions defined by

$$W^{(i)}(\Omega) \equiv \sum_j |\langle j|\hat{Q}|i\rangle|^2 \delta(\Omega - (E_j - E_i)), \quad (3)$$

where  $\hat{Q}$  denotes a probing operator which connects the initial and the final eigenstates  $|i\rangle$  and  $|j\rangle$ . In many cases of interest, the initial state  $|i\rangle$  is set to the ground state of the system  $|gs\rangle$  which belongs to the  $A_1$  symmetry class, in which case the index  $(i)$  is dropped. The response function shows the distribution of the state  $\hat{Q}|i\rangle$  over the energy eigenstates  $\{|j\rangle\}$ . If, for instance, the initial state  $|i\rangle$  has a simple structure as in the ground state of the harmonic oscillator, the state  $\hat{Q}|i\rangle$  and the response function will simply reflect the structure of the probe operator  $\hat{Q}$ . We consider operators depending only on a single variable, say  $\hat{x}$ , to see how the irregular behavior of the wave functions controlled by the parameter  $k$  may be reflected in the response function. One may rewrite the response function (3) in the form of the time-correlation function

$$W^{(i)}(\Omega) = \frac{1}{2\pi} \int_{-\infty}^{\infty} dt e^{i\Omega t} \langle \hat{Q}(\hat{x}(t))^{\dagger} \hat{Q}(\hat{x}(0)) \rangle_i, \quad (4)$$

where  $\langle \rangle_i$  denotes the expectation value in the initial state  $|i\rangle$ . The probe  $\hat{Q}$  is written as a function of the operator

$$\hat{x}(t) \equiv e^{iHt} \hat{x} e^{-iHt} = \hat{x} + \hat{p}_x t - (\hat{x}^3 - k\hat{x}\hat{y}^2)t^2 + \dots, \quad (5)$$

which is the solution of the Heisenberg equation of motion. In Eq.(5) we show also a short time expansion in terms of the operators at  $t = 0$ , e.g.,  $\hat{x}(0) = \hat{x}$ . A corresponding semiclassical expression for Eq. (4) has been fully utilized in the analysis of Refs. [10–14].

It is generally believed that the universal behavior of a dynamical system, i.e., if it is regular or chaotic, emerges in the fluctuation properties of the matrix elements of the operators, while their expectation values are strongly dependent on the specific dynamics of the system. Although the transition matrix elements for a chaotic system are known to generically follow the Porter-Thomas distribution, the energy-strength correlation such as the one contained in response functions is certainly dependent on the specific properties of the dynamics governed by the Hamiltonian. In this latter respect we note that the shape of the response function versus energy is constrained by a number of sum rules [23]. Let us define

$$S_n^{(i)}(\hat{Q}) = \int_{-\infty}^{\infty} d\Omega \Omega^n W^{(i)}(\Omega) = \sum_j (E_j - E_i)^n |\langle j|\hat{Q}|i\rangle|^2 \quad (6)$$

for a given operator  $\hat{Q}$ . The integer  $n$  may in general take negative values (usually for  $i = g.s.$  and  $j \neq g.s.$ ), in which case the sum rule corresponds to the generalized susceptibility of the system. By increasing the value of  $n$  and subtracting the lower moments, e.g., in the form of the shifted moment or of the cumulant, one can regain finer and finer structure of the response function. Although one may recover the response functions by Mellin-transforming the sum rule values, the use of sum rules lies in the fact that in some cases the sum becomes a simple matrix element in the initial state. The latter may be calculated precisely and serves as a check for the accuracy of the calculation. The low  $n$  sum rules, in particular, sometimes become insensitive to the detailed dynamics and constrain the gross behavior of the response functions.

As a probe  $\hat{Q}$  of the response we first consider the operator  $\hat{x}^2$  with an arbitrary initial state  $|i\rangle$ . We then fix  $|i\rangle = |gs\rangle$  and adopt the operator  $\hat{Q}_q \equiv e^{iq\hat{x}}$  which is closely related to an excitation of the system by an external probe characterized by momentum transfer  $q$  (and length scale  $1/q$ ). The operator  $\hat{x}^2$  may be regarded as a long wavelength part of  $\hat{Q}_q$ , and is similar to the  $E2$  operator of electromagnetic transitions. By changing the value of  $q$  in  $\hat{Q}_q$ , one can study in principle long as well as short distance structure of the matrix elements.

In the actual calculation we consider only the operators symmetric under the reflection about  $x$ - and  $y$ -axes and also about the line  $x = y$ , i.e.,

$$\tilde{Q} \equiv (\hat{Q})_{A_1} = \frac{1}{4}(\hat{Q}(\hat{x}) + \hat{Q}(-\hat{x}) + \hat{Q}(\hat{y}) + \hat{Q}(-\hat{y})), \quad (7)$$

where the arguments are explicitly written to show the dependence on the coordinates. For the initial state  $|i\rangle$  in the class  $A_1$  this implies that in Eq. (3) only the states  $j$  belonging to the  $A_1$  symmetry class contribute.

### A. Response to the $\hat{x}^2$ Probe

We first study the response function for the  $\hat{x}^2$  probe. A typical example of the response to this probe is given in Fig.1. Here we show the response  $W^{(i)}(\Omega = E - E_i)$  for the  $i=500$ th initial state as a function of the energy  $E$  for

$k=0.2$  and  $0.6$ . For other initial states the main features are similar. We immediately see that the response consists of three clusters of strengths for both  $k=0.2$  and  $0.6$ : Largest strength lies at  $E = E_i$  with almost no other strength close to this peak, while two other clusters are located around  $E = E_i \pm \Delta$ , where  $\Delta$  is slightly less than  $2\omega_0$ , the expected value for a simple harmonic oscillator. For  $k = 0.2$ , the strengths are concentrated on a few states, while strengths are distributed over some energy range for  $k = 0.6$ . We now introduce creation and annihilation operators  $a_x^\dagger$ ,  $a_x$ , etc., of the oscillator quanta with frequency  $\omega_0$ , and decompose the operator  $\tilde{x}^2$  as

$$\tilde{x}^2 = D_0 + D_2^\dagger + D_2; \quad D_0 \equiv \frac{1}{2\omega_0}(\hat{n}_x + \hat{n}_y + 1), \quad D_2^\dagger \equiv \frac{1}{4\omega_0}(a_x^\dagger{}^2 + a_y^\dagger{}^2). \quad (8)$$

One may then be tempted to assign the  $E = E_i$  peak to the response to the operator  $D_0$ , and two other clusters around  $E = E_i \pm \Delta$  to the operators  $D_2^\dagger$  and  $D_2$ , respectively. Figure 2 (a) and (b) show the response to the operator  $D_0$  for  $k = 0.2$  and  $0.6$ , respectively. Although the state  $D_0|i\rangle$  is not proportional to  $|i\rangle$ , the fragmentation of the strength is restricted to only a few states in both cases. More important is the mixing in the state  $D_2^\dagger|i\rangle$ . Figure 2 (c) and (d) show the response to the operator  $D_2^\dagger$  for the  $i = 500$ th state. The distribution of strengths is considerably different between  $k = 0.2$  and  $k = 0.6$  cases. Strengths for  $k = 0.2$  are seen to concentrate on a few states, while those for  $k = 0.6$  are distributed over many states.

The above features may be quantified by studying the number of principal components (NPC). The NPC for a normalized state  $|\alpha\rangle$  in terms of a complete set of orthonormalized states  $\{|j\rangle\}$  is defined as:

$$N_{\text{pc}}^{(\alpha)} \equiv \left( \sum_j (\langle j|\alpha\rangle)^4 \right)^{-1}. \quad (9)$$

The NPC becomes unity when the strengths are concentrated in a single eigenstate, while becomes  $N_{\text{tot}}$  when the strengths are equally distributed over the whole  $N_{\text{tot}}$  eigenstates. Figure 3 shows the NPC of the state  $D_0|i\rangle$  (with a suitable normalization) for each eigenstate  $|i\rangle$  as a function of  $E_i$ , where the set  $\{|j\rangle\}$  has been taken to be the eigenstate of the Hamiltonian. The NPC takes values  $1 \sim 1.5$  in most cases and decreases as the energy increases. General trend is not much different for  $k = 0.2$  and  $k = 0.6$ . The situation is drastically different if we study the NPC for the state  $D_2^\dagger|i\rangle$  (again normalized) as seen in Fig. 4. For  $k = 0.2$ , the NPC remains small and does not show a marked energy dependence, while for  $k = 0.6$ , the NPC shows a rapid increase as a function of energy and takes a quite large value. We thus find that the  $D_2(D_0)$  part of the operator  $\tilde{x}^2$  is sensitive(Insensitive) to the characteristic changes in the dynamics governed by the parameter  $k$ .

There is another measure to see the difference between the two cases,  $k = 0.2$  and  $k = 0.6$ , which can be obtained from the response function associated with  $\tilde{x}^2$ . In Fig. 5 the fraction of strengths (omitting the one for  $E = E_i$ ) exhausted by two major states carrying largest strengths for each initial state  $|i\rangle$  is plotted against  $E_i$ . For  $k=0.2$  more than 60% of the total strengths is exhausted by the two major states and the distribution of the fraction is almost independent of the initial energy  $E_i$ , while for  $k = 0.6$  they carry less than 50% and this fraction decreases as a function of the initial state energy. Since the dominant part of the strength associated with the operator  $D_0$  is contained in the initial state  $|i\rangle$  and is omitted here, Fig. 5 shows the characteristics for the response to the operator  $D_2^\dagger$  (and  $D_2$ ) in accordance with the results from NPC.

These studies imply that it depends strongly on the choice of the probe whether the difference in the character of the dynamics, namely regular or chaotic, may be easily seen in the response function. In the present case, the difference in the dynamics is not apparent for the probe  $D_0 \sim x^2 + p_x^2$ , while it becomes quite significant for  $D_2 \sim x^2 - p_x^2$  which is a probe, in a sense, ‘orthogonal’ to the unperturbed oscillator Hamiltonian  $\sim D_0$ . The response function for the probe  $\tilde{x}^2$  shows both characteristics.

## B. Response to the Probe $\hat{Q}_q$

We now consider the response function for  $\hat{Q}_q = e^{iq\hat{x}}$ . We fix here the initial state to be the ground state. In this case the response is closely related to the situation of physical interest such as the inelastic electron scattering from the target in the ground state, where  $q$  gives the momentum transfer on the target. The symmetrized probe for  $\hat{Q}_q$  is given by  $\tilde{Q}_q \equiv (\hat{Q}_q)_{A_1} = \frac{1}{4}(e^{iq\hat{x}} + e^{-iq\hat{x}} + e^{iq\hat{y}} + e^{-iq\hat{y}})$ . The response functions  $W(q, \Omega \equiv E - E_{gs})$  (for  $\hat{Q}_q$ ) and  $\tilde{W}(q, \Omega)$  (for  $\tilde{Q}_q$ ) are calculated in terms of the elementary matrix element  $Q_{nm}(q) \equiv \langle n|e^{iq\hat{x}}|m\rangle$  for a one-dimensional harmonic oscillator between the states with quanta  $n$  and  $m$ , which is given by

$$Q_{nm}(q) = i^\alpha e^{\frac{1}{2}z} z^{\frac{1}{2}\alpha} \sqrt{\frac{n!}{(n+\alpha)!}} L_n^\alpha(z) \quad (m \geq n), \quad (10)$$

where  $\alpha \equiv m - n$ ,  $z \equiv q^2/2\omega_0$  and  $L_n^\alpha(z)$  denotes the associated Laguerre polynomial. The functions  $Q_{nm}(q)$  are calculated from recursion relations.

We consider several  $q$  values corresponding to different resolution of the probe, the small  $q$  limit being related to the long-wavelength probe  $\hat{x}^2$  above. On the other hand, for large  $q$  values the operator resolves a fine structure of the system and the main strength of the response lies at high energies. If we use the short-time expansion in Eq. (5) at this high  $\Omega$  region, we can rewrite Eq. (4) for the probe  $\hat{Q}_q$  using the Baker-Campbell-Hausdorff formula as

$$W(q, \Omega) \simeq \frac{1}{2\pi} \int dt e^{i(\Omega - q^2/2)t} \langle e^{-iq\hat{p}_x t + \dots} \rangle_{gs}, \quad (11)$$

where the dots denote operators with higher powers of  $t$ . The expression shows that the response is peaked at the quasielastic energy  $q^2/2$  and has a width increasing with  $q$  and with, e.g., the momentum spread in the ground state. This holds precisely for a simple harmonic oscillator Hamiltonian, while in general is modified by anharmonicity effects. The limiting form of response at large  $q$  has been used to extract momentum distribution of complex system in terms of  $y$ -scaling analysis [24]. In our case, as noted earlier, the model space of diagonalization limits the value of  $q$  around 50 with the corresponding limit  $\sim 1/q$  in the resolution of the wave function. This is much smaller than the length parameter  $1/\sqrt{\omega_0}$  of our oscillator basis. For the quartic oscillator the length scale will be modified from the simple oscillator value. One may define the characteristic length scale in the ground state by  $\bar{x}_{gs} \equiv (\langle gs | \hat{x}^2 | gs \rangle)^{1/2}$ . Calculated values of  $\bar{x}_{gs}^{-1}$  are 1.64 for  $k = 0.2$  and 1.57 for  $k = 0.6$ . Thus the operator at, say  $q = 20$ , probes already a fairly fine structure of the system compared with the length scale of the ground state. The fact that the state  $\hat{Q}_q | gs \rangle$  has an oscillation length scale  $1/q$  also explains the occurrence of the quasielastic peak: The typical oscillation length scale of the harmonic oscillator wave function at energy  $E \sim n\omega_0$  is  $\sqrt{\langle x^2 \rangle}/n \sim 1/\sqrt{E}$  which becomes  $\sim 1/q$  in the region  $E \sim q^2/2$ . Thus, the state  $\hat{Q}_q | gs \rangle$  will have the largest overlap with the states in the quasielastic region producing a peak in the response.

Let us now consider the sum rules. Low  $n$  values of the sum  $S_n \equiv S_n^{(0)}(\hat{Q}_q)$  for the unsymmetrized probe are explicitly calculated to give  $S_0 = 1$ ,  $S_1 = \frac{1}{2}q^2$ ,  $S_2 = \frac{1}{4}q^2(q^2 + \frac{8}{3}E_{gs})$ , etc., where the last sum rule is obtained from the virial theorem. For the symmetric probe the sum  $\tilde{S}_n \equiv S_n^{(0)}(\tilde{Q}_q)$  is not analytically obtained but is given by the expectation values as:

$$\tilde{S}_0 = \frac{1}{4} \langle (1 + \cos q(\hat{x} + \hat{y}))(1 + \cos q(\hat{x} - \hat{y})) \rangle_{gs}, \quad \tilde{S}_1 = \frac{1}{16} q^2 \langle 2 - \cos 2q\hat{x} - \cos 2q\hat{y} \rangle_{gs}, \quad \text{etc.} \quad (12)$$

It is useful to consider the limiting values for  $q \rightarrow 0$  or  $\infty$ :

$$\tilde{S}_0 \rightarrow 1, \quad \tilde{S}_1 \rightarrow \frac{1}{8} q^4 \langle \hat{x}^2 + \hat{y}^2 \rangle_{gs} \quad : \quad \text{for } q \rightarrow 0, \quad (13)$$

$$\tilde{S}_0 \rightarrow \frac{1}{4}, \quad \tilde{S}_1 \rightarrow \frac{1}{8} q^2 \quad : \quad \text{for } q \rightarrow \infty, \quad (14)$$

where the values at  $q \rightarrow \infty$  are obtained under the assumption that the wavelength  $1/q$  is much smaller than the typical length scale of the ground state wave function. These values are used to check the accuracy of the calculation within our model space, especially the one at large  $q$  which requires the matrix elements Eq.(10) with large  $n$ . Note that these values are almost independent of  $k$ , and the numerical calculation confirms that the  $k$ -dependence is small indeed. It turned out that the limiting values (14) for the sum rule are satisfied already at  $q \simeq 10$ . In view of Eq. (12) this result implies that the ground state expectation values of  $\cos q\hat{x}$ , etc., are almost zero, i.e., the resolution at  $q \simeq 10$  is already sufficiently fine for the ground state in accordance with the estimate given above. For higher  $n$  values the dependence of  $\tilde{S}_n$  on  $k$  is expected to become larger. Thus the gross structure of the response such as the total strength  $\tilde{S}_0$  and average energy  $\tilde{S}_1/\tilde{S}_0$  is rather insensitive to the values of  $k$ . Detailed structure related to high  $n$  values of  $\tilde{S}_n$  should reflect the dynamics.

Figure 6 shows the response function  $\tilde{W}(q, \Omega)$  at  $q = 10, 30$  and  $50$ . The gross structures at a given  $q$  are similar for both  $k = 0.2$  and  $0.6$ , and follow the behavior suggested earlier in this section: Not only the central energy follows  $\Omega = q^2/2$  but the width of the response increases almost linearly with  $q$ . This should come out exactly from the sum rule if one had employed an unsymmetrized probe  $\hat{Q}_q$ . Fine structure of the response, on the other hand, is quite different for the two cases. For  $k = 0.2$  the response has a rather simple regular structure: at  $q = 30$ , for instance, the response is a superposition of a few structures with different sizes, each of which is centered around  $q^2/2 = 450$  and is similar to the response of a harmonic oscillator given by

$$W_{\text{ho}}(q, \Omega) = \sum_n \delta(\Omega - n\omega_0) f_n\left(\frac{q^2}{2\omega_0}\right), \quad f_n(z) \equiv \frac{1}{n!} z^n e^{-z}. \quad (15)$$

In fact, by inspecting the wave functions one finds that these structures are related to the strong transition matrix elements of uncoupled (i.e.,  $k = 0$ ) quartic oscillators which are integrable. In contrast, for  $k = 0.6$  the simple structure disappears and the values of the strength change drastically from one state to the other, although one can still see even at  $q = 50$  a structure of the regularly spaced spikes as seen for  $k = 0.2$ .

For chaotic systems such as represented by random matrix theories, the amplitude distribution of wave functions or the matrix element distribution of an operator is known to follow the Porter-Thomas distribution. This may be contrasted to regular systems, where in many cases the quantum number imposes a selection rule of allowed transitions. Our result of response functions is in accordance with this generic behavior as far as the energy-strengths correlation is disregarded. In Fig. 7 we show the strength distribution of the response function for  $k = 0.2$  and  $0.6$  at  $q = 30$ . For  $k = 0.6$  the distribution follows the Porter-Thomas form given by the dashed line and is quite different from that for  $k = 0.2$ .

The question then arises: What is the nature of the persisting regular structure in the response functions of Fig. 6 for  $k = 0.6$ . This structure becomes more visible if one introduces a normalized response function defined by

$$W_{\text{normalized}}(q, \Omega) \equiv \frac{W(q, \Omega)}{\bar{W}(q, \Omega)} \bar{\rho}(\Omega), \quad (16)$$

where  $\bar{W}$  and  $\bar{\rho}$  are respectively the response and the level density smoothed over energies. For the smoothing we employed the method of Strutinsky [26] with the smoothing width of 20. This normalization procedure removes the gross structure effect of the response as constrained by the low order sum rules and enhances the embedded fine structure [22]. Figure 8 shows the normalized response for  $k = 0.2$  and  $0.6$ . They show that the strengths in the regular spikes for  $k = 0.2$  are mostly redistributed for  $k = 0.6$  to produce smaller and smaller strengths to fill up the background, although one can still see the equidistant structure. The latter may be called an intermediate structure following Ref. [27]. This energy-strength correlation in the response function has been washed out in the strength distribution.

The presence of an intermediate structure can be detected also in the response correlation function  $C(\epsilon)$  defined by

$$C(\epsilon) \equiv \int dE \tilde{W}(q, E) \tilde{W}(q, E + \epsilon). \quad (17)$$

For equidistant structures such as the one for the free response (15), the correlation function gives again the regular pattern with the same spacing, e.g.,

$$C_{\text{free}}(\epsilon) = \sum_{n, n'} \delta(\epsilon - (n' - n)\omega_0) f_n(z) f_{n'}(z) = \int \frac{dt}{2\pi} e^{i\epsilon t} e^{2z(1 - \cos \omega_0 t)}, \quad (18)$$

with  $z \equiv q^2/2\omega_0$  and  $f_n$  of Eq.(15). Figure 9 shows the correlation function for the response function at  $q = 30$ . In the actual calculation we used the normalized response function (16) in order to remove the gross shape effect and used the level number displacement  $\delta i$  instead of the energy displacement  $\epsilon$ . The resultant correlation function was then smoothed with a smoothing width  $\Delta i = 4$ . We find the oscillator pattern arising from the intermediate structure in the response function for both  $k = 0.2$  and  $0.6$ .

To understand why there still remains the intermediate structure even in the chaotic case, let us investigate the nature of the peak levels in some detail. We first pick up the peak levels carrying the largest strength among neighboring levels in the response function. For  $k = 0.2$  the assignment of peak levels can be done without difficulty, while for  $k = 0.6$  there may be an ambiguity. The qualitative results of the following analysis are however independent of this ambiguity.

We first studied the NPC's of these peak levels in terms of the basis states (i.e.,  $|j\rangle = |n_1, n_2\rangle_{\text{ES}}$  in Eq.(2)), and found that they are markedly smaller than NPC's for other levels. This implies that the mixing of the basis states in these peak levels is smaller than other states. The nature of the peak levels may become clear from Fig. 10, where we plot the quantity

$$A_n^{(i)} \equiv \langle i | |\hat{n}_x - \hat{n}_y| / (\hat{n}_x + \hat{n}_y) | i \rangle. \quad (19)$$

Here, black points correspond to the peak levels and bars indicate the average values over neighboring levels. For  $k = 0.2$ , the values of  $A_n^{(i)}$  for peak levels are nearly 0.9, almost twice of those for other levels. For  $k = 0.6$ , although it is not so evident as for  $k = 0.2$ , the values for peak levels are larger than the average. These facts strongly indicate that the peak levels are associated with the basis states of the type  $|0, m\rangle_{\text{ES}}$ , although considerably affected by the mixing with other states for  $k = 0.6$ . In fact, these basis states are the only states excited by the probe  $\tilde{Q}_q$  for a simple oscillator Hamiltonian.

We may study the above results from the opposite direction. In Fig.11 we show the NPC of Eq.(9) for the basis state  $|\alpha\rangle \equiv |n_1, n_2\rangle_{\text{ES}}$  by taking the eigenstates  $|i\rangle$  of the Hamiltonian for the states  $|j\rangle$  in Eq.(9). The abscissa is the basis number  $\alpha$ , and the basis state type  $|0, m\rangle_{\text{ES}}$  is denoted by crosses. For both  $k$ -values the basis states of the type  $|0, m\rangle_{\text{ES}}$  have the smallest NPC values, which shows that these basis states have the smallest spreading width caused by the mixing with other basis states. Thus the fact that there remains an intermediate structure in the response function may be restated in the doorway state picture [28]: The probe  $\tilde{Q}_q$  excites first the doorway states  $|0, m\rangle_{\text{ES}}$  which will then mix with other states causing the spreading of the strengths. As the spreading width for these specific states are smaller than the level spacing between the doorway states, the intermediate structure emerges even in the chaotic case.

Since the states  $|0, m\rangle_{\text{ES}}$  may correspond to the classical isolated periodic orbits along the  $x$  and  $y$  axis, the relation between the intermediate structure in the response function and the scar [7] may be an interesting problem. Suppose that an initial wave packet  $|\phi(0)\rangle$  is located at some point of the closed orbit having the period  $T$ . The wave packet will then semiclassically evolve along the closed orbit and will return to the initial position at each time interval  $T$ . Accordingly, the overlap of the wave packet at time  $t$  with the initial wave packet  $|\langle\phi(0)|\phi(t)\rangle|$  will have peaks at  $t = nT$ , where  $n$  is an integer. The value of these peaks will decay due to the instability of the closed orbit like  $\exp(-\lambda/2t)$ , where  $\lambda$  denotes the Lyapunov exponent of the closed orbit [7]. Taking the state  $\hat{Q}_q|gs\rangle$  as the initial wave packet  $|\phi(0)\rangle$ , the response function is nothing but the Fourier transform of the overlap  $|\langle\phi(0)|\phi(t)\rangle|$ . Therefore, the intermediate structure with peak level spacing  $D = 2\pi/T$  and the spreading width of the peaks  $\gamma = \lambda$  may emerge in the response function if the condition  $\gamma/D \leq 1$  is satisfied. In the present model, the period of the closed orbits along the  $x$ - and  $y$ - axes does not depend on the parameter  $k$  and is given by  $T = \frac{1}{\sqrt{2\pi}}\Gamma(\frac{1}{4})^2 \simeq 5.24$  at  $E = 1/2$ . Numerical calculation also shows that the Lyapunov exponents for these closed orbits at  $E = 1/2$  are  $\lambda \simeq 0.53$ , and 0.92 for  $k = 0.2$  and 0.6, respectively. The values of  $\gamma/D$  are then given by 0.44 and 0.77 for  $k = 0.2$  and 0.6, respectively, both of them being smaller than unity. Note that  $\gamma/D$  is independent of the energy. Thus, the existence of the intermediate structure may be explained also from the semiclassical point of view.

#### IV. SUMMARY

In this paper we studied properties of the response functions for a coupled quartic oscillator with several probes with a special attention to the difference between the regular and the chaotic cases.

As a first example, we took the response to the probe  $\hat{x}^2$ . Since the response function is determined by the probe as well as the nature of the wave functions of the system, we must pay attention also to the character of the probe. For instance, the operators for which the diagonal matrix element becomes a main component are not adequate to see the difference of the dynamics. For the operator  $\hat{x}^2$ , it can be decomposed like Eq. (8), and the operator  $D_0$  has such a character, while for the operators  $D_2^\dagger$  and  $D_2$  the non-diagonal matrix elements are important. Therefore, by removing the strengths associated with the operator  $D_0$  we can see the difference of the response between the chaotic and the regular cases, namely more spreading of strengths for the chaotic case, which can be quantified with the number of principal components.

Next, we considered the response to the probe  $\hat{Q}_q = e^{iq\hat{x}}$ . The response function at a given momentum transfer  $q$  is related to the time-correlation function of the operator with a resolution  $1/q$  in the coordinate space. It was shown that the gross structure of the response function is similar for the chaotic and the regular cases as constrained by global sum rules. On the other hand, the difference is reflected on the fluctuation, as seen in the strength distribution (the histogram of strengths). Moreover, we detected the intermediate structure (i.e., typical energy scales) even in the chaotic case which can not be expected for the random-matrix model. We found that the existence of the intermediate structure is due to the fact that the spreading width of the doorway states is smaller than the level spacing of the doorway states, and also indicated its relation to the scar phenomenon. It would be interesting to study this structure from a different point of view, e.g., the semiclassical theory of responses [10–13] based on the periodic orbits.

In this paper for the sake of simplicity we restricted the discussion to the transitions between the states belonging to the same symmetry class. In the realistic situation, however, the transition connecting states with different symmetry classes may also occur at same time. It is well known that the level spacing statistics drastically changes when we consider the levels belonging to different symmetry classes simultaneously. Thus, it is also interesting to see what happens for the response function to the probe connecting different symmetry classes.

The authors thank M.Matuso for valuable discussions. They thank also P.Schuck for a discussion about the semiclassical description of response functions.

- 
- [1] M.V. Berry, in *Chaotic Behavior in Deterministic Systems*, edited by G. Iooss, R.H.G. Helleman and R. Stora (North-Holland, 1983), p.171.
  - [2] O. Bohigas and M.-J. Giannoni, in *Mathematical and Computational Methods in Nuclear Physics*, edited by J.S. Dehesa, J.M.G. Gomez, and A. Polls, Lecture Notes in Physics Vol.219 (Springer, Berlin, 1984), p.1.
  - [3] T.A. Brody *et al.*, Rev. Mod. Phys. **53**, 385 (1981).
  - [4] T. Guhr, A. Müller-Groeling and T.A. Weidenmüller, Phys. Rep. **299**, 189 (1998).
  - [5] M.C. Gutzwiller, *Chaos in Classical and Quantum Mechanics* (Springer, 1990); J. Math. Phys. **12**, 343 (1971).
  - [6] C.E. Porter and R.G. Thomas, Phys. Rev. **104**, 83 (1956);  
C.E. Porter, *Statistical Theories of Spectra: Fluctuations*, (Academic Press, 1965).
  - [7] H.J. Heller, Phys. Rev. Lett. **53**, 1515 (1984); Lec. Note in Phys. **263**, 162 (1986).
  - [8] M. Feingold and A. Peres, Phys. Rev. A **34**, 591 (1986).
  - [9] Y. Alhassid and R.D. Levine, Phys. Rev. Lett. **57**, 2879 (1986);  
Y. Alhassid and M. Feingold, Phys. Rev. A **39**, 374 (1989).
  - [10] M. Wilkinson, J. Phys. A **20**, 2415 (1987).
  - [11] B. Eckardt *et al.*, Phys. Rev. A **45**, 3531 (1992).
  - [12] B. Mehlis and M. Wilkinson, J. Phys. Cond. Matter **9**, 3277 (1997).
  - [13] B. Mehlis and K. Richter, Phys. Rev. Lett. **80**, 1936 (1998);  
B. Mehlis, Phys. Rev. E **99**, 390 (1999).
  - [14] V.N. Kondratyev, Phys. Lett. A **179**, 209 (1993).
  - [15] P. Schuck *et al.*, Prog. Part. Nucl. Phys. **22**, 181 (1989); Phys. Lett. **118B**, (1982) 237.
  - [16] L. McCauley, Phys. Reports **189**, 225 (1990).
  - [17] A. Carnegie and I.C. Percival, J. Phys. A **17**, 801 (1984).
  - [18] H.-D. Meyer, J. Chem. Phys. **84**, 3147 (1986).
  - [19] Th. Zimmermann *et al.*, Phys. Rev. A **33**, 4334 (1986).
  - [20] B. Eckhardt, G. Hose, and E. Pollak, Phys. Rev. A **39**, 3776 (1989).
  - [21] O. Bohigas, S. Tomsovic, and D. Ullmo, Phys. Rep. **223**, 43 (1993).
  - [22] H. Aiba and T. Suzuki, Phys. Lett. A **201**, 319 (1995);  
H. Aiba, S. Mizutori, and T. Suzuki, Phys. Rev. E **56**, 119 (1997).
  - [23] O. Bohigas, A.M. Lane and J. Martorell, Phys. Rep. **51**, 267 (1979).
  - [24] G.B. West, Phys. Rep. **18**, 263 (1975);  
D.B. Day *et al.*, Ann. Rev. Nucl. Part. Sci. **40**, 357 (1990).
  - [25] E.J. Austin and M. Wilkinson, Europhys. Lett. **20**, 589 (1992).
  - [26] V.M. Strutinski, Nucl. Phys. **A95**, 420 (1967).
  - [27] A.M. Lane, R.G. Thomas and E.P. Wigner, Phys. Rev. **98**, 693 (1955).
  - [28] V.F. Weiskopf, Phys. Today **14**, 18 (1960).

FIG. 1. Response to the probe  $\tilde{x}^2$  for the initial state  $|i = 500\rangle$  as a function of the energy  $E$  for  $k = 0.2$  (a) and  $0.6$  (b). Contained levels in the displayed energy regions are 459th to 542th for  $k = 0.2$  and 462th to 554th for  $k = 0.6$ .

FIG. 2. Response to the operator  $D_0$  for the initial state  $|i = 500\rangle$  as a function of energy  $E$  for  $k = 0.2$  (a) and  $0.6$  (b), and the one for the operator  $D_2^\dagger$  for  $k = 0.2$  (c) and  $0.6$  (d).

FIG. 3. The NPC  $N_{pc}^{(i)}$  for the state  $D_0|i\rangle$  as a function of the energy of the initial eigenstate  $E_i$  for  $k = 0.2$  (a) and  $0.6$  (b).

FIG. 4. Same as Fig. 3 but for  $D_2^\dagger$ .

FIG. 5. The fraction of the  $\tilde{x}^2$  strengths (omitting the one for  $E = E_1$ ) carried by the two major states to the total strengths is plotted for each initial state  $|i\rangle$  as a function of the initial state energy  $E_i$ .



FIG. 6. Response function  $\tilde{W}(q, E)$  for  $k = 0.2$  at  $q = 10$  (a), 30 (c), and 50 (e) and for  $k = 0.6$  at  $q = 10$  (b), 30 (d), and 50 (f). Note the changes in the scale of the vertical axis.

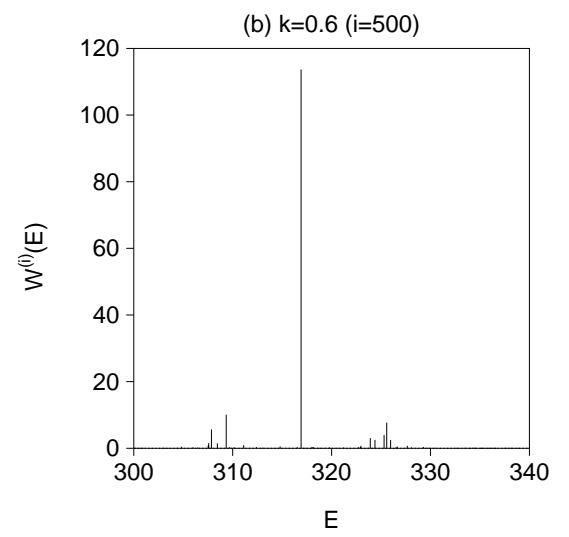
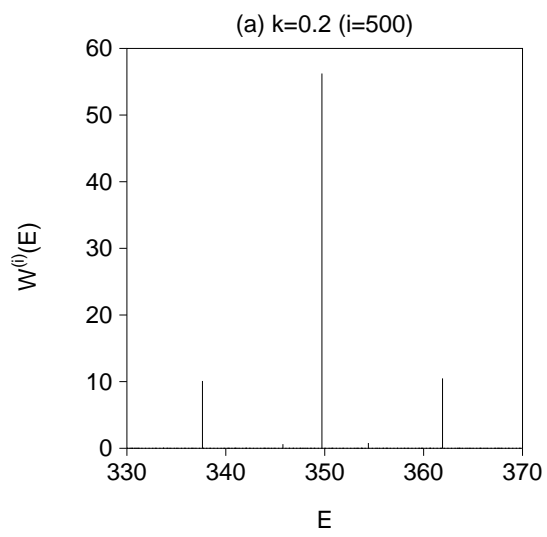
FIG. 7. Strength distribution  $P(S^{1/2})$  of the matrix element  $S \equiv |\langle j|\tilde{Q}_q|gs\rangle|^2$  at  $q = 30$  for  $k = 0.2$  (a) and 0.6 (b). Strengths are normalized as Eq. (16). Dashed line shows the Porter-Thomas distribution.

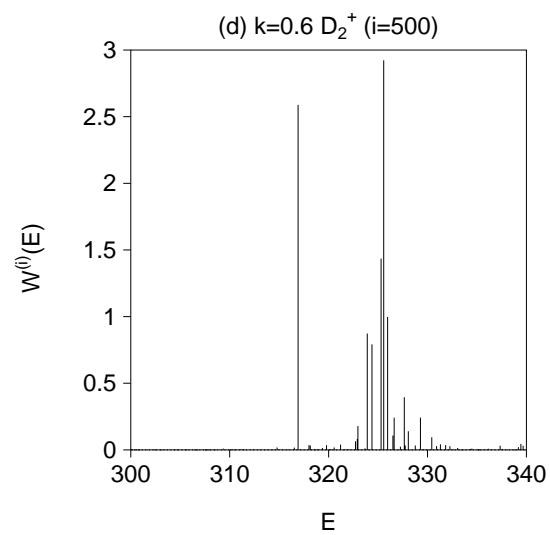
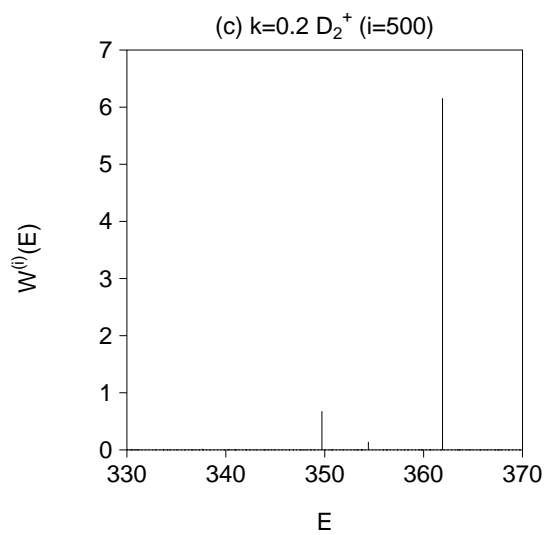
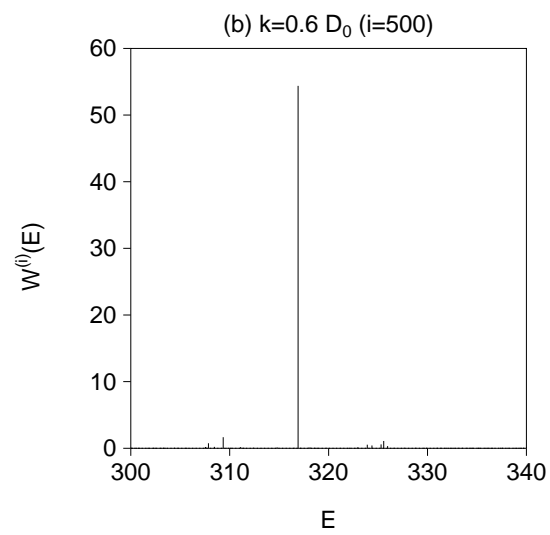
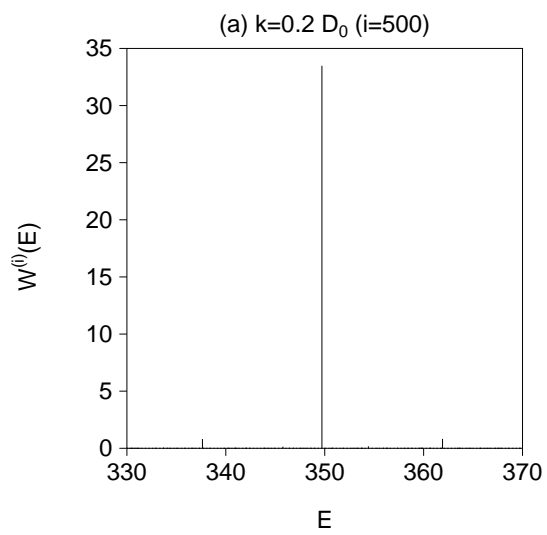
FIG. 8. The normalized response function Eq. (16) at  $q = 30$  for  $k = 0.2$  (a) and 0.6 (b). Compare with the responses at  $q = 30$  shown in Fig. 6.

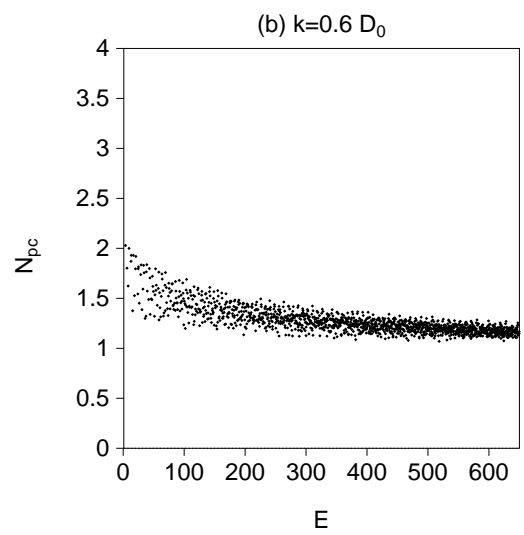
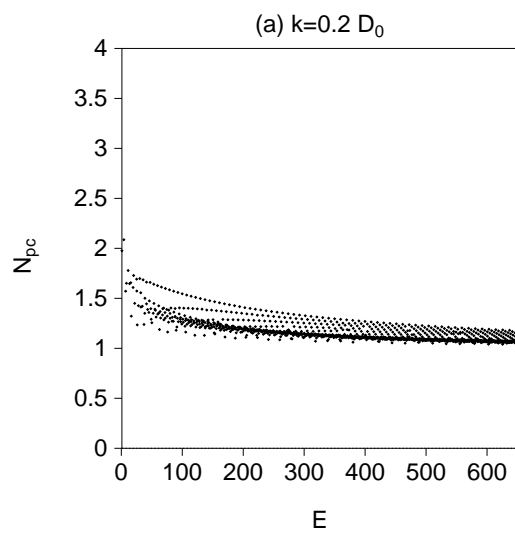
FIG. 9. Smoothed correlation function  $C(\delta i)$  for the normalized response function to the probe  $\tilde{Q}_q$  with  $q = 30$  as a function of the level number displacement  $\delta i$  for  $k = 0.2$  (a) and 0.6 (b). Smoothing width  $\Delta i = 4$  is adopted.

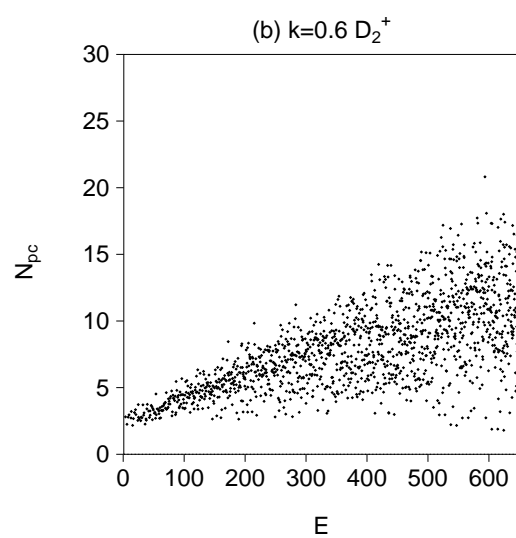
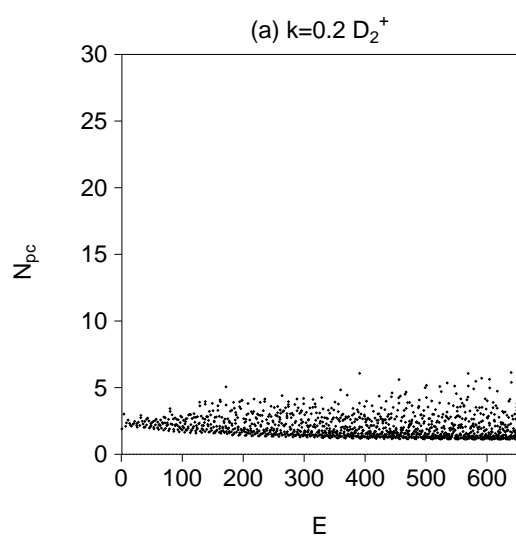
FIG. 10. The quantity  $A_n^{(i)}$  for  $k = 0.2$  (a) and 0.6 (b). Black points denote the peak levels for the probe  $\tilde{Q}_q$  with  $q = 30$  and bars show the average over neighboring levels.

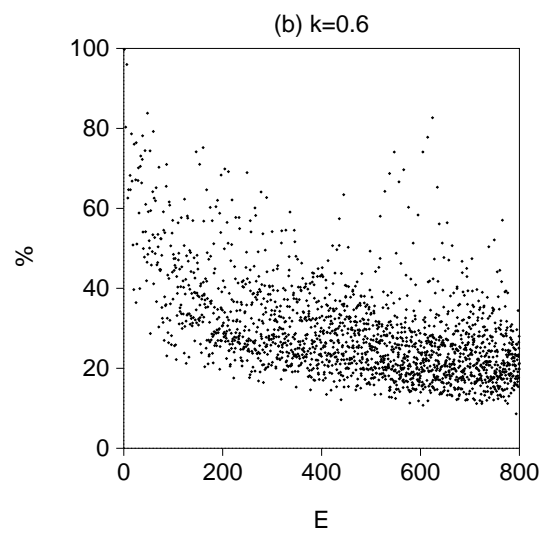
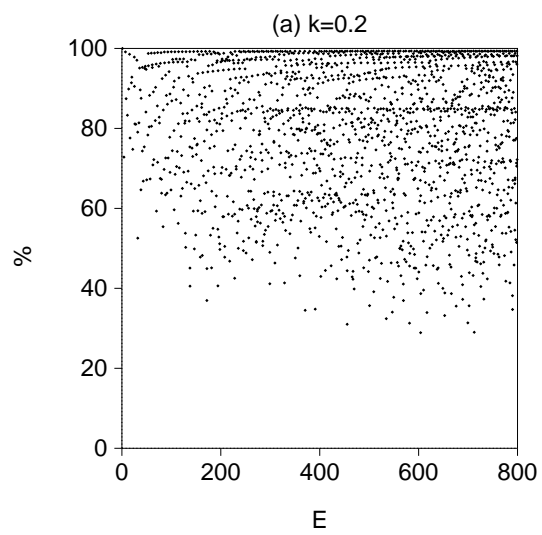
FIG. 11. The NPC  $N_{\text{pc}}^{(\alpha)}$  for basis state  $|\alpha\rangle$  belonging to the symmetry class  $A_1$  for  $k = 0.2$  (a) and 0.6 (b). Horizontal axis shows the level number of the basis state  $|\alpha\rangle$ . Cross points correspond to the basis states type  $|0, m\rangle_{\text{ES}}$ .

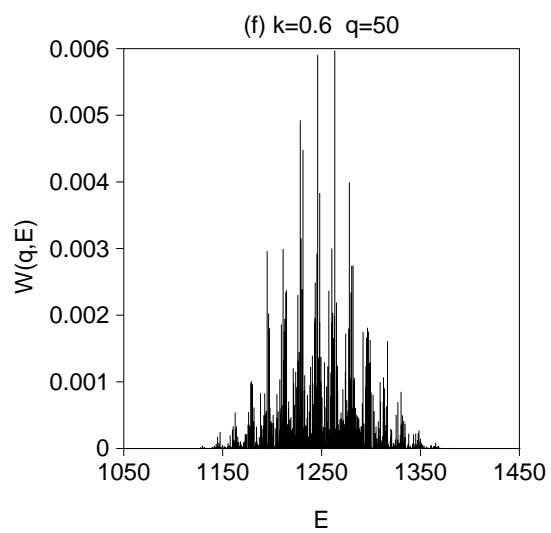
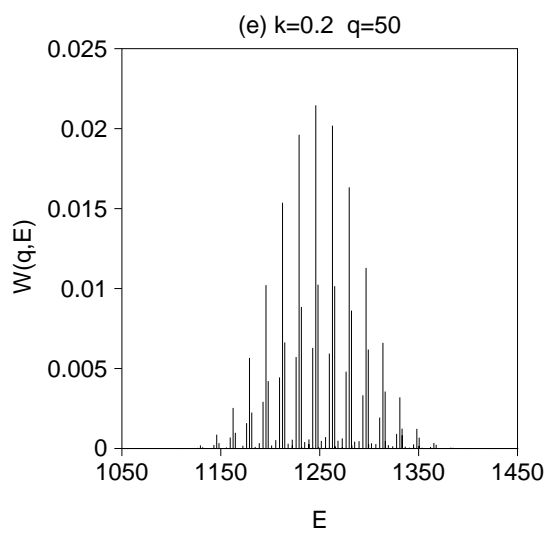
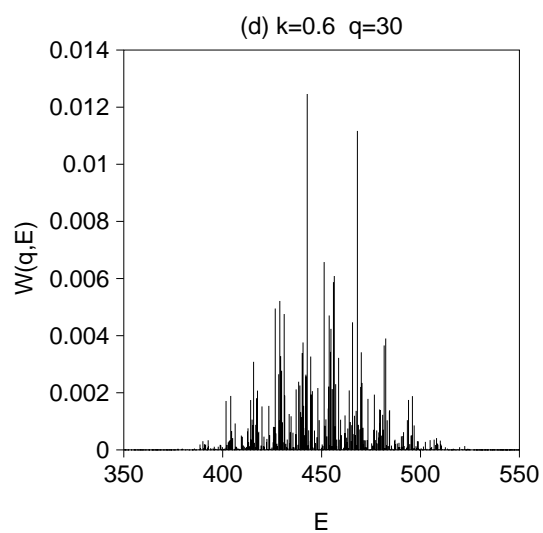
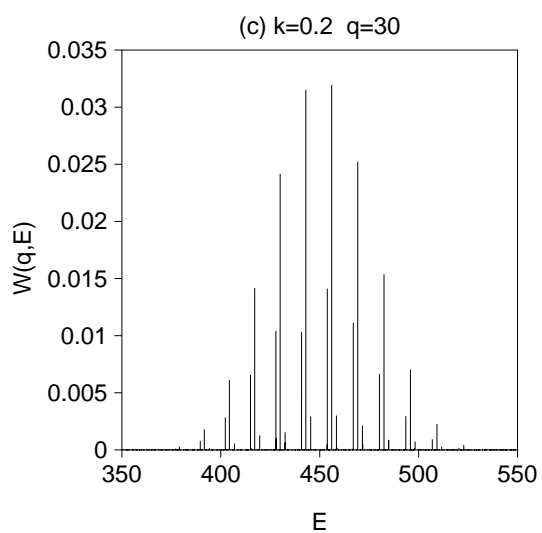
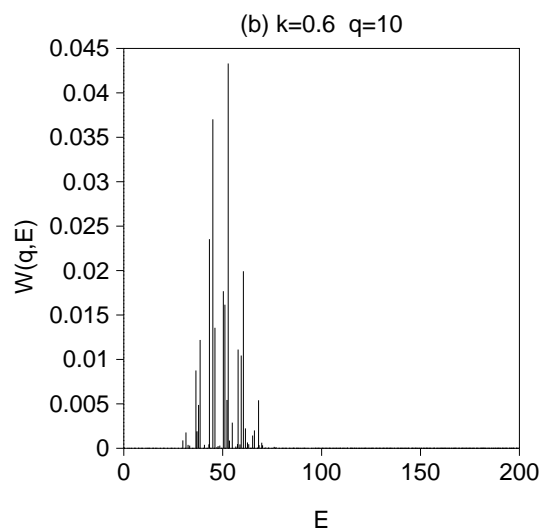
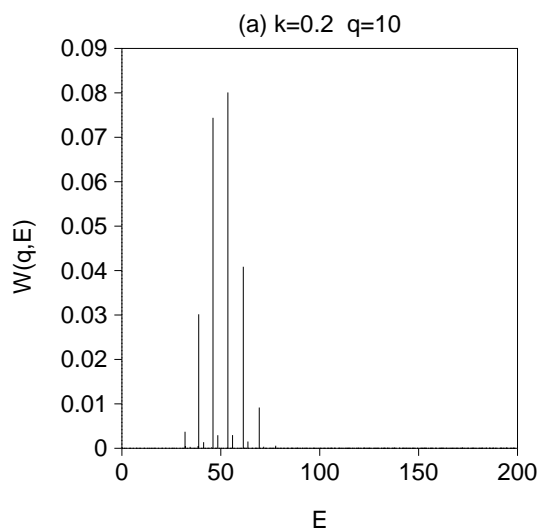


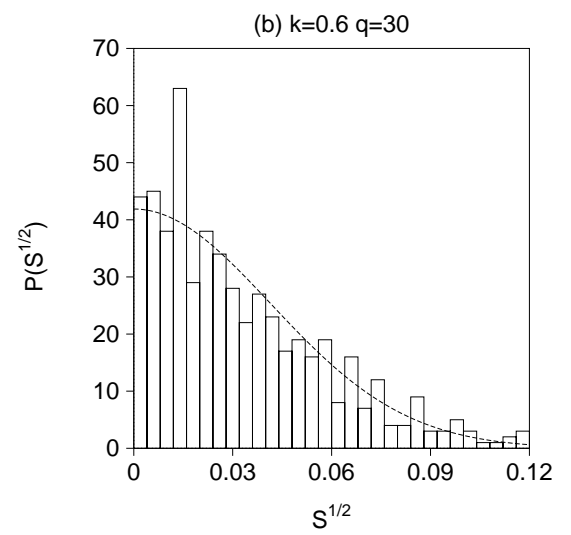
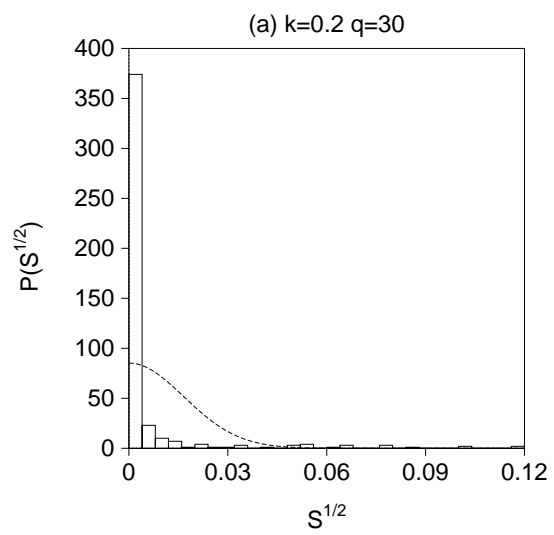




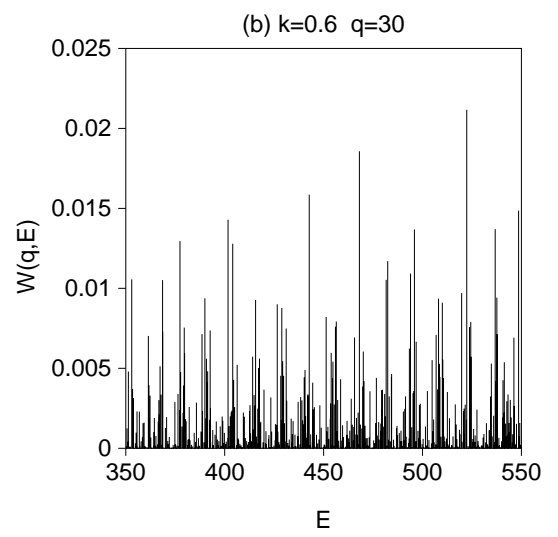
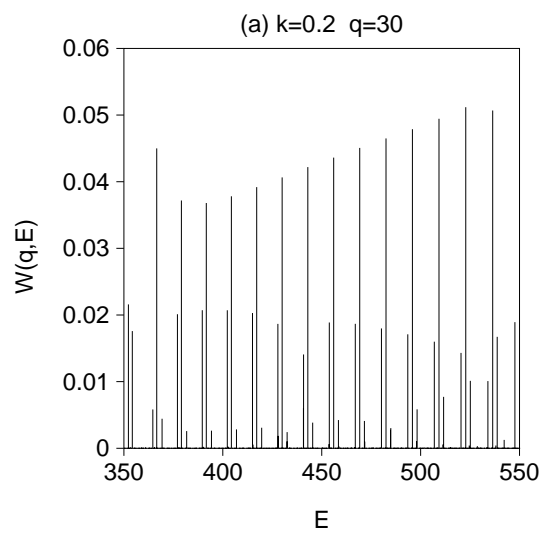


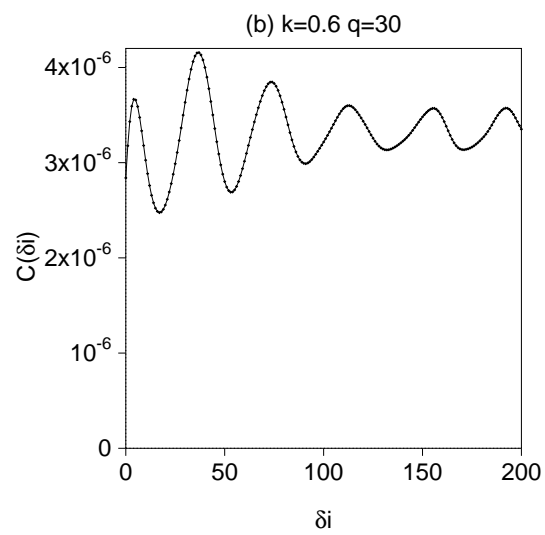
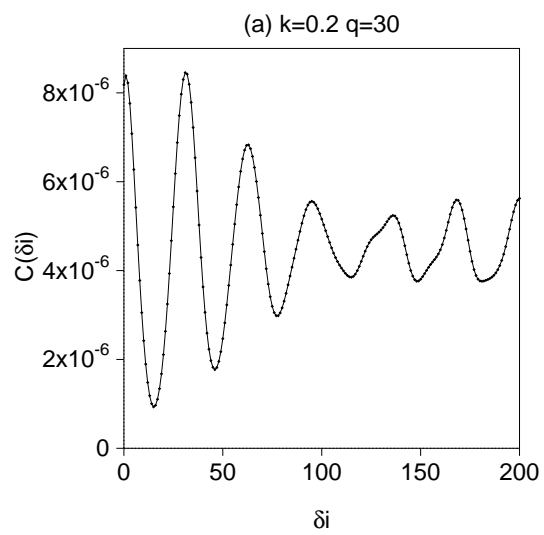


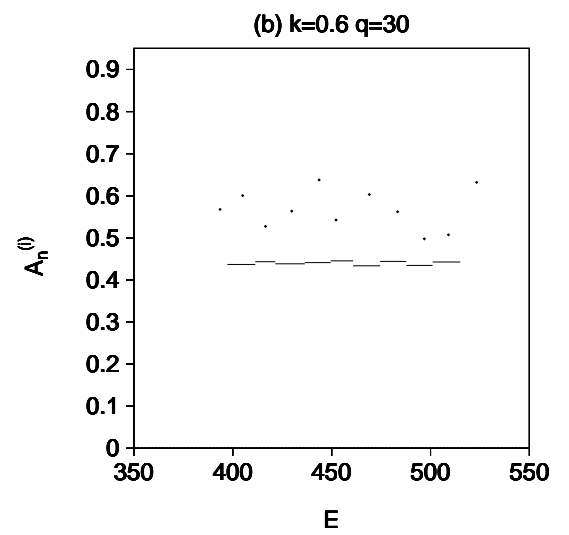
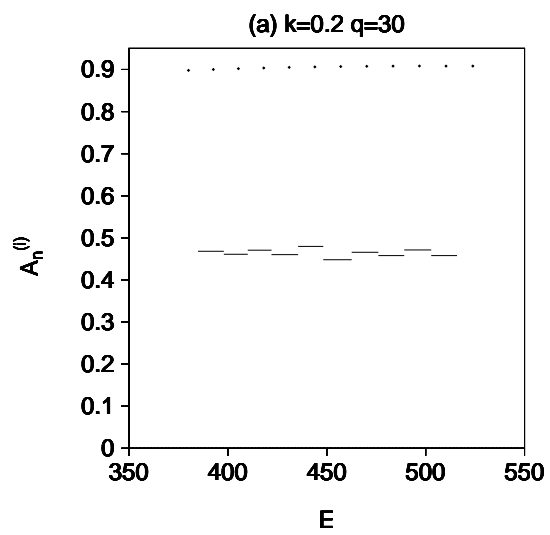




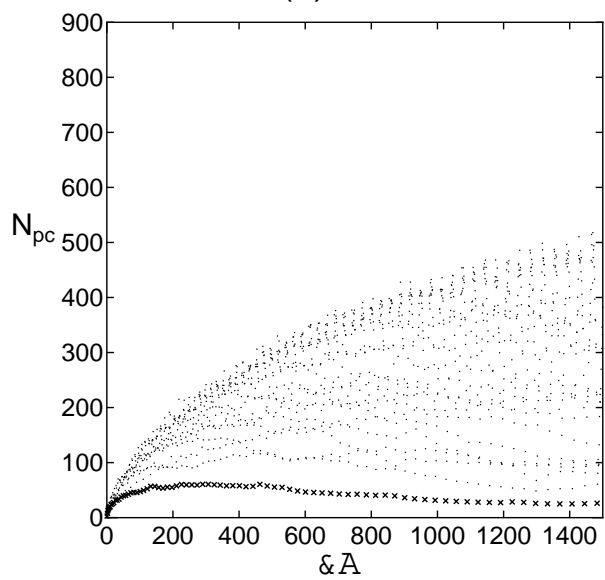








(a)  $k=0.2$



(b)  $k=0.6$

